NEW SIMULATIONS ON MICROBUNCHING INSTABILITY AT TTF2

Yujong Kim* and Klaus Flöttmann, DESY, D-22603 Hamburg, Germany
Dongchul Son and Y. Kim, The Center for High Energy Physics, Daegu 702-701, Korea

Abstract

Microbunching instability can be induced by collective self-fields such as longitudinal space charge, coherent synchrotron radiation, and geometric wakefields when an electron bunch has current density modulation and/or energy modulation at the upstream of a bunch compressor (BC). Since electron beam parameters such as slice and projected emittances, slice energy spread, and peak current are diluted by the microbunching instability, FEL performance is also influenced by the instability. In this paper, we describe new start-to-end (S2E) simulations with 1.5 million macroparticles on the microbunching instability at the TESLA Test Facility Phase 2 (TTF2) linac.

INTRODUCTION

Recently it was reported that the microbunching instability can be induced at TESLA Test Facility Phase 2 (TTF2) and LCLS linear accelerators by density modulations in the gun driving laser pulse, and the main source of the instability is longitudinal space charge (LSC) [1]-[4]. To estimate the strength of the instability, we define a gain parameter as the ratio of the normalized amplitude of a density modulation at the final position to that of the initial modulation. In the case of TTF2, the analytically estimated maximum gain of the microbunching instability after the second bunch compressor (BC3) is about 320 when an initial density modulation with about 2.0 ps period is applied at the upstream of the first TESLA accelerating module (ACC1) [1]. In 2003, we performed S2E simulations with 50000 macroparticles to estimate its realistic maximum gain. In those simulations, ELEGANT code was used to consider CSR at two BCs and to consider the geometric short-range wakefields at all TESLA accelerating modules, and ASTRA code was also used to consider space charge force through entire regions from the cathode to the end of TTF2 linac [4], [5]. But due to a strong numerical noise, it was difficult for us to estimate an exact gain for modulations with a small modulation amplitude. To reduce the numerical noise, we have performed new S2E simulations with 1.5 million macroparticles. TTF2 layout is shown in Fig. 1, and detail simulation methods and TTF2 machine parameters are described in references [5] and [6]. In this paper, we only focus in modulations with 2.0 ps period to estimate the realistic maximum gain of the microbunching instability at TTF2 linac. Other simulation results with different modulation periods can be found in reference [5].

* E-Mail : Yujong.Kim@DESY.de, URL : http://TESLA.DESY.de

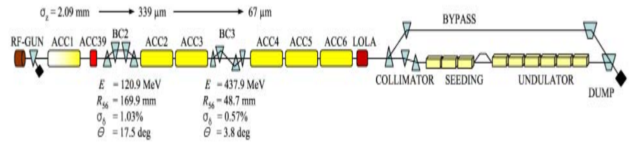

Figure 1: TTF2 layout for the nominal operation.

S2E SIMULATION RESULTS

Recently, we found that a strong artificial microbunching is generated after BC if we choose too many BINs in ELEGANT CSR algorithm with small simulating macroparticles. We can control this artificial microbunching by increasing macroparticles and by choosing a proper BIN number. After TTF2 BC3, we also meet such a strong artificial microbunching even though we simulate no modulation case with 1.5 million macroparticles as shown in Fig. 2. Only when BIN is reduced down to about 125, we can damp the artificial microbunching. After considering Nyquist sampling theorem and the artificial microbunching instability, we have chosen 125 as the BIN number in the ELEGANT CSR algorithm, which is large enough to study 2.0 ps modulations.

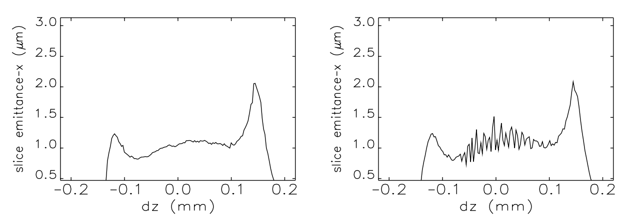

Figure 2: After BC3, S2E simulation results for no modulation case with 1.5 million macroparticles. Here used BINs are 125 (left) and 500 (right).

To investigate the amplification of an initial modulation at the end of the first bunch compressor (BC2), five different initial density modulations with 2.0 ps period and $\pm 1.25\%$, $\pm 2.5\%$, $\pm 5.0\%$, $\pm 7.5\%$, and $\pm 10\%$ amplitudes are assumed at the cathode as shown in Fig. 3(left) [4], [5]. In the case of a modulation with $\pm 1.25\%$ amplitude, its initial density modulation is almost damped down at 0.5 m downstream from the cathode by the fast space charge oscillation and the strong Landau damping as shown in Figs. 3(right) and 4(left) [2]-[5]. Although we can see the same damping for modulations with higher amplitudes, there are still undamped modulations at the core region as

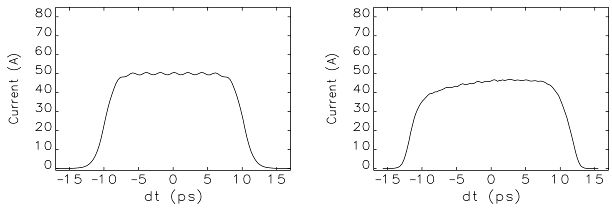

Figure 3: Initial current profile at the cathode for a modulation with 2.0 ps period and $\pm 1.25\%$ amplitude (left), and its current profile at 0.5 m downstream from the cathode (right).

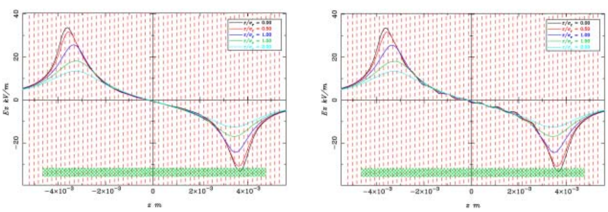

Figure 4: At 0.5 m downstream from the cathode, longitudinal electric field due to space charge force for two initial modulations with $\pm 1.25\%$ (left) and $\pm 10\%$ (right) amplitudes. Here r is the radial position in a bunch [5].

shown in Fig. 4(right). Since 2D space charge force generates variations in the longitudinal electric field (or local energy spread) at the head and tail, initial density modulations are effectively smeared at the head and tail region.

According to theory, LSC induces energy modulation in a linac or in a drift space if current density is modulated at the upstream path [1], [2]. In our simulations, however, induced energy modulation before BC2 is small enough because initial modulation amplitude is effectively damped by the fast space charge oscillation and the strong Landau damping at the low energy region as shown in Figs. 3(right), 4(left), and 5(left column). However, in the BC, the undamped density modulation is converted to a new additional energy modulation by CSR, and the induced energy modulation before BC is also converted to a new additional density modulation at the BC because electron path length in the BC depends on its energy via the nonzero dispersion. The energy modulation after BC2, consequently, grows with the same frequency as that of the initial current modulation as shown in Fig. 5, and the current density modulation after BC2 is also amplified as shown in Fig. 6.

However amplification of the current density modulation after BC2 is weak enough as shown in Fig. 6(right column), where the gain of the current density modulation after BC2 is about 1.1 with respect to initial modulations at the cathode. Therefore a single stage bunch compressor does not generate the strong current density modulation.

Since the space charge oscillation and the Landau damping are weak after BC2, the density modulation after BC2 becomes frozen up to BC3. But the energy modulation

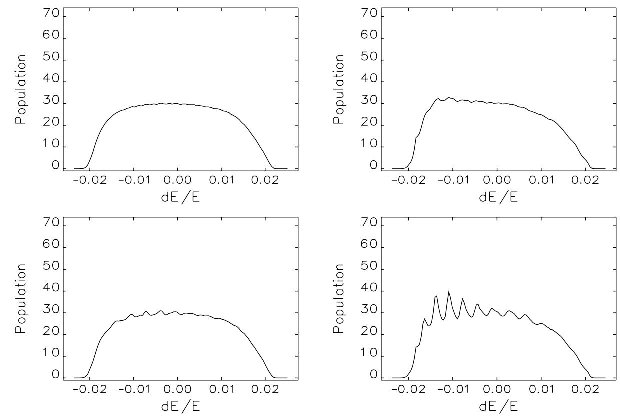

Figure 5: Energy profiles before BC2 (left column) and after BC2 (right column) for two initial modulations with $\pm 1.25\%$ (top row) and $\pm 10\%$ (bottom row) amplitudes at the cathode.

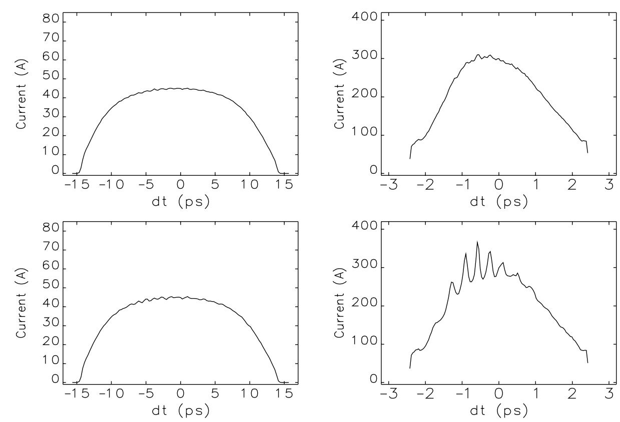

Figure 6: Current profiles before BC2 (left column) and after BC2 (right column) for two initial modulations with $\pm 1.25\%$ (top row) and $\pm 10\%$ (bottom row) amplitudes at the cathode.

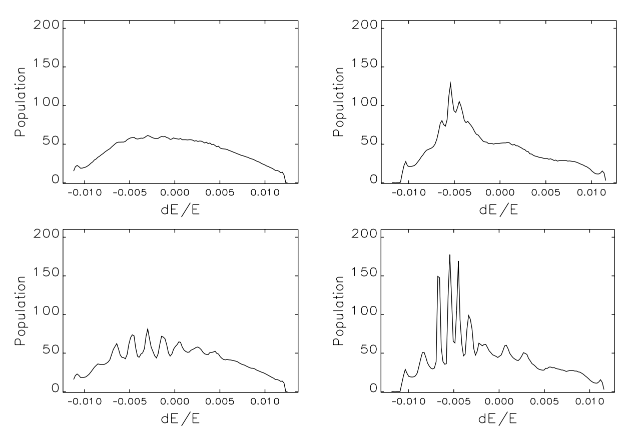

Figure 7: Energy profiles before BC3 (left column) and after BC3 (right column) for two initial modulations with $\pm 1.25\%$ (top row) and $\pm 10\%$ (bottom row) amplitudes at the cathode.

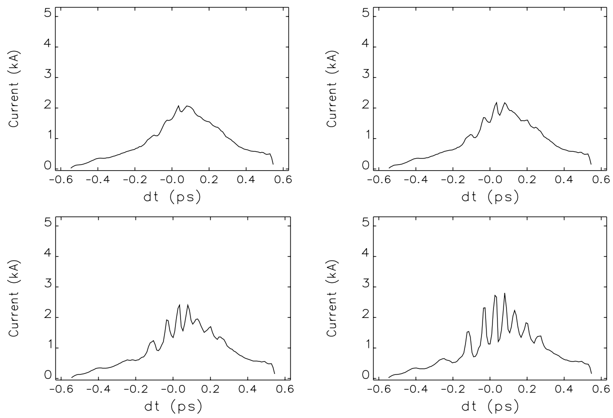

Figure 8: After BC3, current profiles for four initial modulations with $\pm 1.25\%$ (top left), $\pm 2.5\%$ (top right), $\pm 5.0\%$ (bottom left), and $\pm 10\%$(bottom right) amplitudes at the cathode.

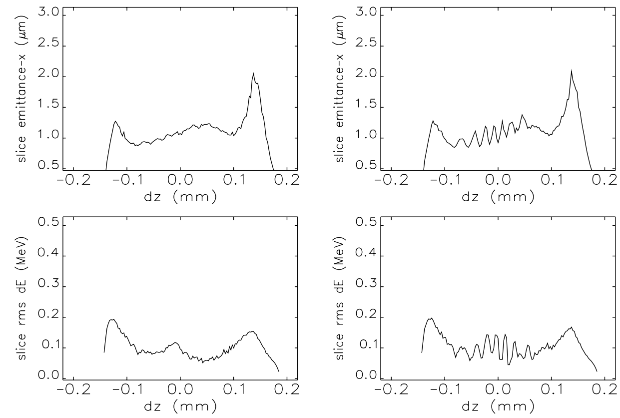

Figure 10: After BC3, slice normalized rms emittance (top row) and slice rms energy spread (bottom row) for two initial modulations with $\pm 1.25\%$ (left column) and $\pm 10\%$ (right column) amplitudes at the cathode.

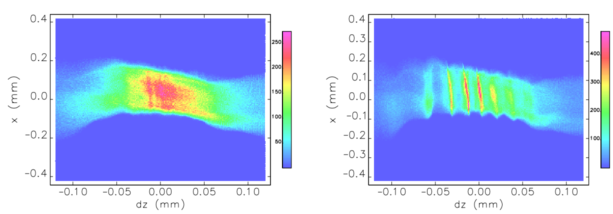

Figure 9: After BC3, 2D histogram for two initial modulations with $\pm 1.25\%$ (left) and $\pm 10\%$ (right) amplitudes at the cathode.

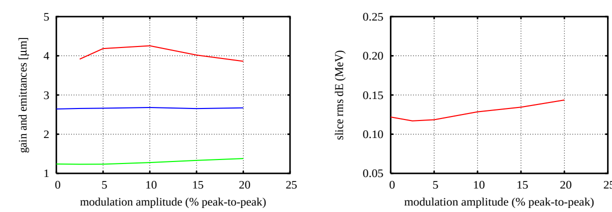

Figure 11: After BC3, (left) red, blue, and green lines indicate the total gain of the microbunching instability in TTF2 linac, projected horizontal emittance, and slice horizontal emittance, respectively. (right) slice rms energy spread.

is continuously accumulated up to the BC3 by LSC and geometric wakefields in the linac as shown in Fig. 7(left column). Since the frozen density modulation is also reconverted to a new additional energy modulation in BC3 by CSR, the energy modulation is reamplified at BC3 as shown in Fig. 7(right column). The current density modulation is also reamplified after BC3 because the accumulated energy modulation is reconverted to a new additional density modulation in BC3 via the nonzero dispersion as shown in Fig. 8. However overall amplification or the gain of the microbunching instability is small enough as shown in Figs. 8, 9, 10, and 11. Specially, a modulation with $\pm 1.25\%$ amplitude does not give any strong amplification as shown in Figs. 8, 9, 10, and 11.

Since CSR becomes stronger as the modulation amplitude or nonlinearity in the current profile is increased, modulation amplitudes in slice rms energy spread, slice normalized rms emittance, and peak current are slightly increased, and projected normalized rms emittance is also slightly increased as shown in Figs. 8, 10, and 11 [4], [7]. After BC3, the gain of the microbunching instability with respect to the initial density modulation at the cathode is around 4 for all modulation amplitudes as shown in Fig. 11. Here all slice parameters are estimated from the peak of those parameters within ± 0.1 mm core region.

SUMMARY

By increasing macroparticles up to 1.5 million particles and by choosing a proper BIN number in ELEGANT CSR algorithm, we can effectively damp the artificial microbunching due to the numerical noise. The estimated gain of the microbunching instability after the second BC in the TTF2 linac is only around 4 for all modulations with 2.0 ps period. Even though we have a modulation with $\pm 10\%$ amplitude at the cathode, all slice parameters are much lower than those parameters for the TTF2 nominal operation [6]. Therefore we expect that we may not need any special designed damping system in the TTF2 linac.

REFERENCES

[1] E.L. Saldin *et al.*, TESLA-FEL 2003-02.

[2] Z. Huang *et al.*, SLAC-PUB-10334, 2004.

[3] Juhao Wu *et al.*, SLAC-PUB-10430, 2004.

[4] Yujong Kim *et al.*, Nucl. Inst. and Meth. A, in press.

[5] http://www.desy.de/∼yjkim/FEL03P02.pdf

[6] TTF FEL team, DESY report No. TESLA-FEL 2002-01.

[7] R. Li, Nucl. Inst. and Meth. A, **475** (2001) 498.